

# Unitary (semi)causal quantum-circuit representation of black hole evaporation

Bogusław Broda

21 February 2024

**Abstract** A general structure of unitary evolution (evaporation) of the black hole, respecting causality imposed by the event horizon (semicausality), has been derived and presented in the language of quantum circuits. The resulting consequences for the evolution of the corresponding entanglement entropy and the entropy curve have been determined. As an illustration of the general scheme, two families of qubit toy models have been discussed: tensor product models and controlled non-product models.

## 1 Introduction

The black hole (BH) information paradox formulated in [1] is still an interesting, unsolved, and inspiring problem. Recent progress, starting with the two famous papers made in 2019, [2] and [3], consists in the computation of the von Neumann entropy of the radiation emitted by BHs in the framework of some specific models of quantum gravity. It appears that in these models, the shape of the entropy curve is essentially given by the Page curve [4]. Instead, in the present work, we concentrate on the description of the unitary evolution and evaporation process of BHs directly in terms of qubits, according to the ideas reviewed by e.g. [5]. Extensive literature with some 50 references to various qubit models is given in [6] (see also proposals in [7, 8, 9]). Despite these large studies, it seems that the important issue of properly understood causality in the process of transport of quantum information in the presence of the BH event horizon has been largely ignored. The aim of our work is to at least partially fill the gap.

The paper consists of two parts, and the whole analysis is performed in the language of quantum circuits. In the first part (Section 2), we implement the concept of causality that is, in our opinion, most natural for the description of the process of evolution (and evaporation) of a BH. Namely, taking into account the role played by the BH event horizon, the kind of causality appropriate in this case is given by the (already existent in literature) notion of *semicausality*. The semicausality in turn imposes some restrictions on the structure of unitary evolution and, in consequence, on the evolution of entropy and (in a graphic presentation) on the entropy curve. In the second part of the paper (Section 3), we present and analyze two large families of unitary qubit toy models that explicitly implement the idea of (semi)causality. The first family comprises some tensor product models, whereas the second one is a non-product generalization of the first family with a small number of control qubits.

## 2 The general structure of unitary semicausal circuits

In this section, we would like to establish a general structure of unitary transformations governing the evolution of evaporating BHs, which properly respect causality implied by the presence of the BH event horizon. Because of our later needs (see Section 3), the answer will be formulated in the language of quantum circuits. Since unitary transformations (and their corresponding quantum circuits) are supposed to act in regions both outside and inside the BH, restrictions following from causality should be properly encoded in the structure of the circuit. It appears that the version of causality appropriate in the context of a BH is semicausality. In quantum mechanics, the notion of semicausality has a short history. The concept of semicausality first appeared in [10], was analyzed in [11] (see also [12]), and was later discussed by [13] (see also [14]) in the circuit (diagrammatic) representation. One should also note that semicausality has already explicitly appeared in the context of BHs in [15].

Occasionally, we loosely use the term *(semi)causality* instead of semicausality (e.g., in the title) or even causality, but referring to causality in the present paper, we exclusively mean the notion of semicausality (precisely, causality is something different—it is semicausality “valid in both directions”).

### 2.1 Semicausality in quantum circuits

An inherent characteristic property of the BH is its one-way transmission of information (and particles) through its event horizon. This property perfectly harmonizes with the notion of semicausality introduced in the context of quantum mechanics and is phrased in the following way [10]: If a bipartite operation  $\mathcal{E}$  does not enable superluminal signalling from Bob to Alice (denoted in literature as  $B \rightarrow A$ , or similarly), then we say that  $\mathcal{E}$  is semicausal. In the interesting context of the event horizon, Bob should be placed inside the BH, whereas Alice should reside outside the BH. The main result of [11] is a proof of a conjecture by DiVincenzo (mentioned by [10]), which (in physics terms) says that if a device allows no signalling from Bob to Alice (semicausality), we can represent it explicitly as a device involving possibly a particle sent from Alice to Bob but none in the other direction. More precisely (in mathematical terms), let the unitary evolution of the tripartite system BXA be described by the operator  $U^{(BXA)}$ . Then  $U^{(BXA)}$  can be represented by the following product containing unitary operators  $U^{(BX)}$  and  $U^{(XA)}$  [14]:

$$U^{(BXA)} = (U^{(BX)} \otimes 1^{(A)}) (1^{(B)} \otimes U^{(XA)}), \quad (1)$$

where B denotes Bob’s subsystem, X is a “particles’ sent” subsystem, and A denotes Alice’s subsystem. A diagrammatic (circuit in block form) presentation of (1) is depicted in Figure 1a (see [13]). We can also present another, essentially equivalent version of the theorem, which is better suited for our further considerations:

$$U^{(BXA)} = (U^{(BX)} \otimes U^{(A)}) (U^{(B)} \otimes U^{(XA)}), \quad (2)$$

where the additional unitary operators  $U^{(A)}$  and  $U^{(B)}$  only redefine the subsystems A and B after and before the evolution (1), respectively. A diagrammatic version of (2) is presented in Figure 1b.

In the process of BH evaporation (and BH evolution in general), we deal with a continuous flux of particles (e.g., external real “matter” particles and/or Hawking’s virtual ones) constantly crossing the event horizon and entering the BH. Therefore, the formula (1) or (2) should be appropriately generalized, i.e., iterated. Namely, the unitary evolution of the  $N$ -partite system  $X_1 X_2 \dots X_N$  described by the operator  $U^{(X_1 X_2 \dots X_N)}$  should be a (huge, in the BH case) iteration of (2), assuming the form

$$\begin{aligned} U^{(X_1 X_2 \dots X_N)} = & (U^{(X_1 X_2 \dots X_{N-1})} \otimes U^{(X_N)}) \\ & \dots (U^{(X_1 X_2)} \otimes U^{(X_3 \dots X_N)}) (U^{(X_1)} \otimes U^{(X_2 \dots X_N)}) \end{aligned} \quad (3)$$

(see Figure 2), where all the operators  $U^{(\dots)}$  are unitary.

Going from  $N$ -partite (hugely multi-particle, in general) quantum subsystems  $X_1, X_2, \dots, X_N$  of the system  $X$  (here the symbol  $X$  should not be confused with a “particles’ sent” subsystem X from

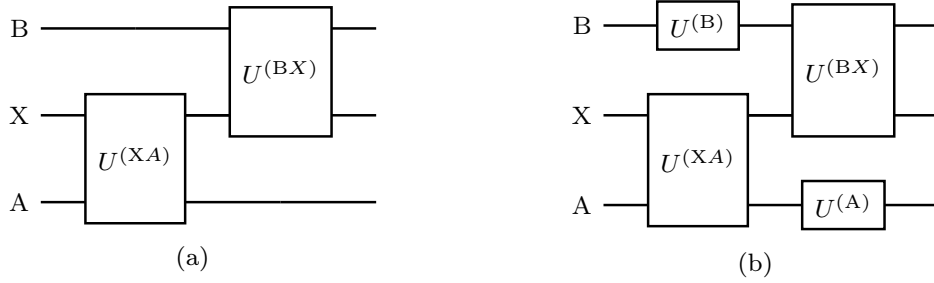


Fig. 1: Diagrammatic representation of the operator  $U^{(BXA)}$  defining the unitary evolution of the tripartite system BXA, where no signalling from Bob (B) to Alice (A) is allowed (semicausality). Transmission of information can only be related to particle(s) (X) sent from Alice (A) to Bob (B), but not in the other direction. Here (a) presents the original version of the operator, given in (1), whereas (b) presents its slightly generalized version (2), which is better suited for our further considerations.

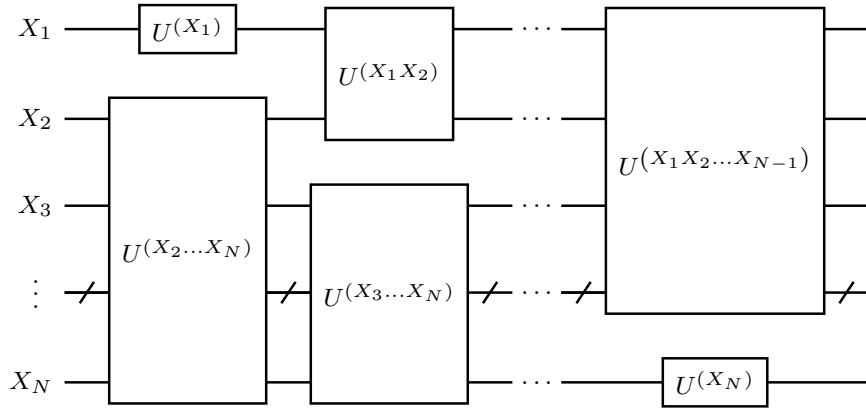


Fig. 2: Diagrammatic representation of the operator  $U^{(X_1 X_2 \dots X_N)}$ , which is an arbitrarily large iteration of the operator  $U^{(BXA)}$  defined in (2) and depicted in Figure 1b.

the beginning of this subsection) to  $n$  qubits  $x_1, x_2, \dots, x_n$  (usually  $n \gg N$ ), we can replace (3) with its (most) fine-grained version

$$U^{(x_1 x_2 \dots x_n)} = \left( U^{(x_1 x_2 \dots x_{n-1})} \otimes U^{(x_n)} \right) \dots \left( U^{(x_1 x_2)} \otimes U^{(x_3 \dots x_n)} \right) \left( U^{(x_1)} \otimes U^{(x_2 \dots x_n)} \right), \quad (4)$$

or equivalently (in a shorter notation) by

$$U = \left( U_{n-1}^{(1)} \otimes U_{n-1}^{(2)} \right) \dots \left( U_2^{(1)} \otimes U_2^{(2)} \right) \left( U_1^{(1)} \otimes U_1^{(2)} \right) \equiv U_{n-1} \dots U_2 U_1, \quad (5)$$

where  $U_k \equiv U_k^{(1)} \otimes U_k^{(2)}$  ( $k = 1, \dots, n-1$ ). The expansion (4) or equivalently (5) can be a bit further generalized to

$$U = U_n \left( U_{n-1}^{(1)} \otimes U_{n-1}^{(2)} \right) \dots \left( U_2^{(1)} \otimes U_2^{(2)} \right) \left( U_1^{(1)} \otimes U_1^{(2)} \right) U_0 \equiv U_n U_{n-1} \dots U_2 U_1 U_0, \quad (6)$$

where the ‘‘external’’ unitary operators  $U_0$  and  $U_n$  have been added in analogy to the generalization (2), and they only redefine the *in* (initial) state  $|\psi_{\text{in}}\rangle$  and the *out* (final) state  $|\psi_{\text{out}}\rangle$ , respectively (see Figure 3). In the context of BH evolution, the operators  $U_0$  and  $U_n$  are supposed to act before the BH forms and after its complete evaporation, respectively.

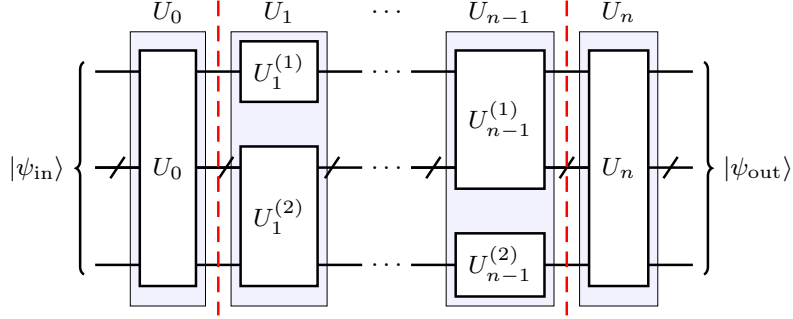


Fig. 3: (Color online) Diagrammatic representation of the unitary evolution operator  $U$  defined in (6), which is a slight generalization of the operator  $U^{(x_1 x_2 \dots x_n)}$  in (4), interpreted as the most fine-grained particle version of the operator  $U^{(X_1 X_2 \dots X_N)}$  given in (3) and depicted in Figure 2. The vertical dashed left line and the right line denote the theoretically earliest moment and the latest one, when the BH is allowed to exist, respectively.

One should stress that according to (5), the decomposition  $\mathcal{H} = \mathcal{H}_k^{(1)} \otimes \mathcal{H}_k^{(2)}$  ( $k = 1, \dots, n-1$ ) of the total Hilbert space  $\mathcal{H}$  onto a product of the two Hilbert spaces  $\mathcal{H}_k^{(a)}$ ,  $a = 1, 2$ , where the superscripts 1 and 2 correspond to the interior and the exterior of the BH, respectively, is “dynamical”. In other words, the decomposition of  $\mathcal{H}$  gradually changes in the course of the (indexed by  $k$ ) evolution of the BH, as depicted in Figures 3 and 4. This observation undermines the validity of the fixed global decomposition of the total Hilbert space  $\mathcal{H}$  in the context of BH evaporation.

## 2.2 Bounds on entanglement entropy

The general situation and the area of our interest between two arbitrary neighbouring unitary blocks  $U_{k-1}$  and  $U_k$  have been presented in Figure 4. The total (pure) state exiting the unitary block  $U_{k-1}$  and next entering  $U_k$  has been denoted by  $|\psi_k\rangle$ . As follows from Figure 4, the configuration in the area between the two pairs of unitary operators,  $U_{k-1} \equiv U_{k-1}^{(1)} \otimes U_{k-1}^{(2)}$  and  $U_k \equiv U_k^{(1)} \otimes U_k^{(2)}$ , gives rise to the four density operators  $\rho_k^{(a)\mp}$ ,  $a = 1, 2$ . Here the signs “-” and “+” denote the LHS and the RHS of the area in Figure 4, respectively, and the values of the superscript  $a$  correspond to the values 1 and 2 in the two decompositions of the Hilbert space  $\mathcal{H} = \mathcal{H}_{k-1}^{(1)} \otimes \mathcal{H}_{k-1}^{(2)}$  and  $\mathcal{H} = \mathcal{H}_k^{(1)} \otimes \mathcal{H}_k^{(2)}$  for the LHS and the RHS, respectively. The entanglement entropy  $\mathcal{S}$  is the von Neumann entropy of the reduced density matrix calculated for one of the four subsystems, which in the block notation of Figure 1b could be denoted by the superscripts B, XA, BX, and A, and which in the current notation of Figure 4 are denoted by the superscripts (1)–, (2)–, (1)+, and (2)+, respectively. Utilizing a well-known equality between the von Neumann entropies in a two-partite division (here denoted by the superscript  $a = 1, 2$ ) of a system in a pure state  $|\psi_k\rangle$  we can skip (on both sides, i.e., for both superscripts “-” and “+”) the superscript  $a = 1, 2$ , i.e.,

$$\begin{aligned} \mathcal{S}(\rho_k^{(1)\mp}) &= -\text{Tr} \left[ \rho_k^{(1)\mp} \ln \rho_k^{(1)\mp} \right] \\ &= -\text{Tr} \left[ \rho_k^{(2)\mp} \ln \rho_k^{(2)\mp} \right] = \mathcal{S}(\rho_k^{(2)\mp}) \equiv \mathcal{S}(\rho_k^\mp) \equiv \mathcal{S}_k^\mp. \end{aligned} \quad (7)$$

By assumption, the unitary evolution (6) is entirely general and only restricted by a single kinematic condition: semicausality. It appears that even though we should not expect too much without any additional dynamic input, some very general results can be derived. Namely, the global (semi)causal structure of the total unitary evolution  $U$  defined in (6) (see Figure 3) implies bounds on the evolution of the entanglement entropy  $\mathcal{S}$ . The evolution of  $\mathcal{S}$  itself can be characterized by the steps (here denoted by  $\mathcal{S}_k^\mp$ )

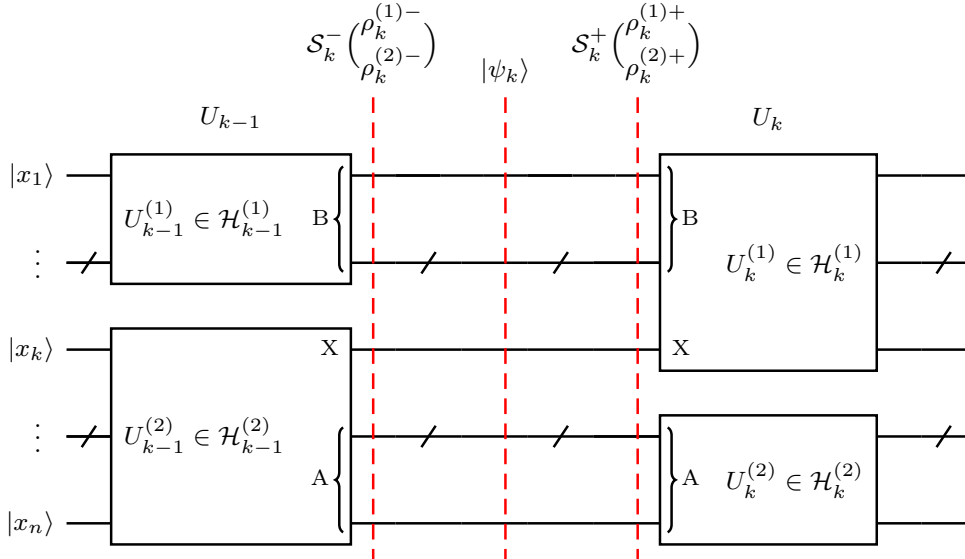


Fig. 4: (Color online) Description of the configuration between two arbitrary neighbouring unitary blocks of Figure 3. The (pure) state between the two blocks  $U_{k-1}$  and  $U_k$  is denoted by  $|\psi_k\rangle$ . In our notation, the correspondence between the reduced density matrices and the subsystems is as follows:  $\rho_k^{(1)-} - (B) \equiv (x_1, \dots, x_{k-1})$ ,  $\rho_k^{(2)-} - (XA) \equiv (x_k, \dots, x_n)$ ,  $\rho_k^{(1)+} - (BX) \equiv (x_1, \dots, x_k)$ , and  $\rho_k^{(2)+} - (A) \equiv (x_{k+1}, \dots, x_n)$  (see (2) and (4)). The entanglement entropy  $S_k^\mp$  is by definition the von Neumann entropy for the reduced density matrix  $\rho_k^{(a)\mp}$  ( $a = 1, 2$ ), where, as it turns out,  $a$  can be arbitrary and thus finally skipped.

$$S_1^- (= 0) \rightarrow S_1^+ \rightarrow S_2^- \rightarrow S_2^+ \rightarrow \dots \rightarrow S_k^- \rightarrow S_k^+ \rightarrow \dots \rightarrow S_{n-1}^+ \rightarrow S_n^- \rightarrow S_n^+ (= 0), \quad (8)$$

where the presence of zeros ( $S_1^- = S_n^+ = 0$ ) should be obvious by virtue of Figure 3. In turn, the bounds on entropy can be derived from the Araki–Lieb version of the triangle inequality [16]

$$|S^{(B)} - S^{(X)}| \leq S^{(BX)} \leq S^{(B)} + S^{(X)}, \quad (9)$$

here written in the notation of Figures 1a or 1b. In particular, for a one-qubit  $X$ , the evolution of the von Neumann entropy is constrained by the inequality (essentially, a version of the triangle inequality)

$$|\Delta S| \equiv |S^{(BX)} - S^{(B)}| \leq \ln 2. \quad (10)$$

Explicitly, (10) is a consequence of the following three inequalities:

$$\begin{cases} 1^{\text{st}} & S^{(BX)} - S^{(B)} \leq S^{(X)}; \\ 2^{\text{nd}} & -S^{(X)} \leq S^{(BX)} - S^{(B)}; \\ 3^{\text{rd}} & S^{(X)} \leq \ln 2, \end{cases} \quad (11)$$

where the  $1^{\text{st}}$  inequality follows from the RHS of the triangle inequality (9), the  $2^{\text{nd}}$  one is a consequence of the LHS of (9), whereas the  $3^{\text{rd}}$  inequality is a bound for the entropy for two-dimensional Hilbert space of the one-qubit subsystem  $X$ . Alternatively, instead of the above reasoning in the part referring to the  $1^{\text{st}}$  and  $2^{\text{nd}}$  inequality in (11) one can ignore the RHS of (9) and using arguments of elementary geometry permute the superscripts in (9) according to  $\begin{pmatrix} (B) & (X) & (BX) \\ (BX) & (B) & (X) \end{pmatrix}$ .

Translating (10) onto “the indexed notation” of (8) (see Figure 4), for each “time” step  $k$  ( $k = 1, \dots, n$ ), we get the inequality

$$|\Delta S_k| \equiv |S_k^+ - S_k^-| \leq \ln 2. \quad (12)$$

The description of the evolution of entropy can be simplified a bit by the fact that entropy is invariant (isometric invariance) with respect to arbitrary unitary transformations (similarity transformations, in general), denoted below by the symbol  $U^{(a)}$  and defined by the operator  $U^{(a)}$  ( $a = 1, 2$ ), of the corresponding density matrix, i.e.,

$$U^{(a)} \left[ S \left( \rho_k^{(a)\mp} \right) \right] \equiv S \left[ U^{(a)} \rho_k^{(a)\mp} \left( U^{(a)} \right)^{-1} \right] = S \left( \rho_k^{(a)\mp} \right). \quad (13)$$

Therefore, in the series (8), we can make the following identifications

$$S_k^+ \equiv S \left( \rho_k^{(a)+} \right) = U_k^{(a)} S \left( \rho_k^{(a)+} \right) = S \left( \rho_k^{(a)-} \right) \equiv S_{k+1}^- \equiv S_k, \quad a = 1, 2, \quad (14)$$

where the first equality follows from 13 and the second one follows from the fact that the unitary transformation  $U_k^{(a)}$  corresponds to the time evolution (shift in indices) operator  $U_k^{(a)}$  (entropy is a constant of motion), i.e., in terms of indices alone,  $U_k^{(a)} : \overset{(a)+}{k} \mapsto \overset{(a)-}{k+1}$ . In consequence, (14) allows us to a bit simplify our notation by skipping the superscripts “+” and “-” as indicated in the last identity in (14). By identifying neighbouring terms according to (14), the series (8) can be substantially simplified and rearranged as follows

$$S_0 (= 0) \rightarrow S_1 \rightarrow \dots \rightarrow S_k \rightarrow \dots \rightarrow S_{n-1} \rightarrow S_n (= 0). \quad (15)$$

Now also (12) assumes a simpler form

$$|\Delta S_k| = |S_k - S_{k-1}| \leq \ln 2, \quad (16)$$

where  $k = 1, \dots, n$ . Iteration of (16) yields the solution

$$S_k \leq k \ln 2 + S_0, \quad (17)$$

or (taking into account the initial condition  $S_0 = 0$ )

$$S_k \leq k \ln 2, \quad (18)$$

or (by virtue of the non-negativity of entropy)

$$0 \leq S_k \leq k \ln 2 \quad (19)$$

(see Figure 5a). In the next step, let us utilize (16) once more. First of all, we can observe that successively inserting the indices  $k = 1, k = 2, \dots, k = n - 1, k = n$  to (16) we obtain the sequence of inequalities  $|S_1 - 0| \leq \ln 2, |S_2 - S_1| \leq \ln 2, \dots, |S_{n-1} - S_{n-2}| \leq \ln 2, |0 - S_{n-1}| \leq \ln 2$ . Solving that sequence of the inequalities, e.g. simply by successive insertions in the order written (the order of the increasing “time”  $k$ ), we obtain (19), but solving it in reversed order (decreasing “time”  $k$ ) yields the inequality

$$0 \leq S_k \leq (n - k) \ln 2. \quad (20)$$

Since the incorporation of semicausality enforces an order in time evolution, one could wonder whether we are allowed to change the order of “time”  $k$ . Fortunately, the “time”  $k$ -inversion amounts to only reversing the order of successive insertions in the process of solving the above set of inequalities, and the semicausality is not at risk. Intuitively, it could also be justified by the observation that even though the theoretical input we use is the notion of semicausality, all diagrams in Figures 1, 2, 3, and 4 look time-symmetric. Alternatively, purely formally, making use of the fact that the time-inversed evolution  $U^\top$  (where the symbol “ $\top$ ” denotes time-inversion) of the given time evolution  $U$  is also time evolution, we could repeat our analysis for the new (time-inversed) evolution  $U^\top = U^{-1}$  obtaining (20). The logical conjunction of (19) and (20) yields our final (double) inequality

$$0 \leq S_k \leq \min(k, n - k) \ln 2, \quad k = 0, 1, \dots, n, \quad (21)$$

which is illustrated (for  $n = 11$ ) by Figure 5b.

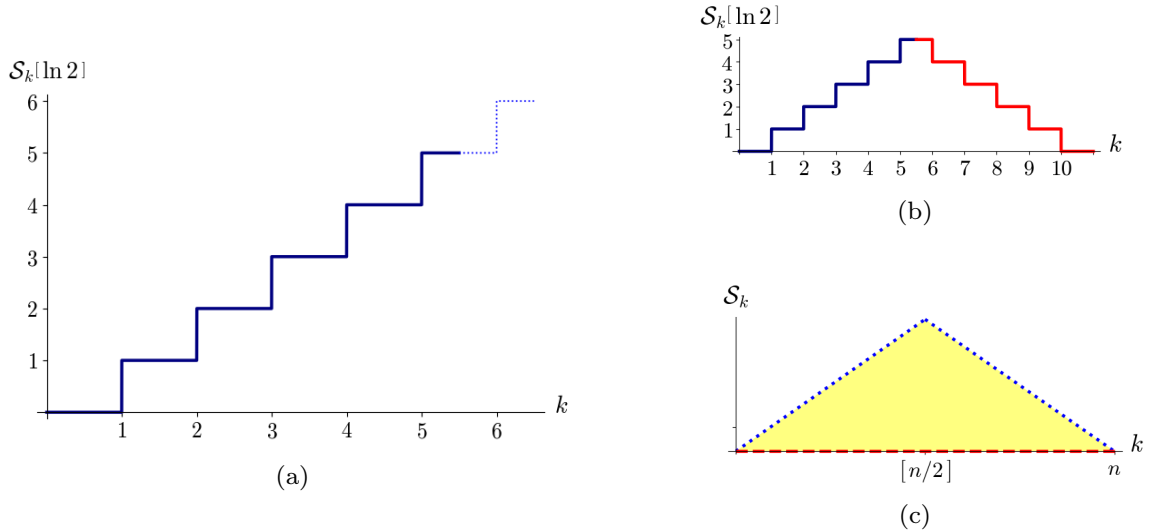


Fig. 5: (Color online) Bounds on entropy curves for unitarily evolving systems, which follow from semicausality. In particular: (a) presents the (beginning part of the) curve of the quickest possible growth of entanglement entropy according to the limitation imposed by (19); (b) takes into account “symmetric” limitations (21) (here  $n = 11$ ); in the limit of a very large  $n$ , the (shaded) triangle in (c) presents an allowed area for any entropy curve for semicausal unitary evolution; here the two upper (dotted) edges of the triangle form a Page-like curve.

### 2.2.1 The entropy curve for (semi)causal evolution

For huge  $n$  according to (21) the lower and the upper bounds for the entropy  $S_k$  can be graphically represented as the lower (dashed) edge and the two upper (dotted) edges of the (shaded) triangle in Figure 5c, respectively. In other words, for any unitary semicausal evolution, the entropy curve  $S_k$  is supposed to satisfy the following *semicausal entropy bound(s)*:

1. The curve  $\mathcal{C}$ , a graphic representation of the function  $S_k$ , should lie inside the shaded triangle ( $\Delta$ ) depicted in Figure 5c ( $\mathcal{C} \subseteq \Delta$ ).
2. Its slope (derivative, in an appropriate continuous limit) should be bounded by the inequality

$$\left| \frac{dS}{dk} \right| \leq \ln 2. \quad (22)$$

(22) is a differential version of (16).

## 3 Examples of semicausal models

To illustrate ideas concerning the (semi)causal structure of unitary models of BH evolution (evaporation) introduced in the previous section, we present two large multiparametric families of qubit toy models: (1) a family of tensor product models defined in Subsection 3.1; (2) a family of controlled non-product models introduced in Subsection 3.2. In Subsubsection 3.1.1 for pedagogical reasons, we start from a very simple three-qubit (3Q) model, which can serve as a building block for subsequent constructions. In Subsubsection 3.1.2, we “tensor exponentiate” the 3Q model, first yielding its tensor square ( $3Q^2$ ), and next, in Subsubsection 3.1.3, its  $m$ -th tensor power ( $3Q^m$ ). In Subsection 3.2 as a less straightforward generalization of the 3Q model, we propose a family of non-product models. In particular, Subsubsection 3.2.1 introduces a four-qubit controlled version of the 3Q model, which we can call the controlled three-qubit (C3Q) model. A (non-product) generalization of the C3Q model to an arbitrarily large number  $n$  of qubits is proposed in Subsubsection 3.2.2. Obviously, by virtue of the

construction, all the introduced models are unitary and semicausal, and in consequence, they satisfy the entropy bounds of Subsection 2.2.

Since all the proposed models of BH evaporation are formulated in a rather formal language of qubits and quantum circuits, some explanations in terms of physics should be given. To begin with, let us observe that there is a direct correspondence between qubit models and two-state spin models. In turn, at least in principle, two-state spin models can be translated (e.g., via the Jordan–Wigner transformation) onto fermion models. Keeping that observation in mind, for our discussion, we can loosely, i.e., ignoring the actual Jordan–Wigner transformation, assume the following convention: the qubit  $|0\rangle$  can be associated to a vacuum state, whereas the qubit  $|1\rangle$  can be associated to a one-particle state.

In physics terms, the picture of the BH evolution depicted in Figure 3 looks as follows. The vertical dashed left line and the right line denote the theoretically earliest moment and the latest one, respectively, when the BH is allowed to exist—no causal restrictions (single vertical boxes  $U_0$  and  $U_n$ ) and then no event horizons. Obviously, in more realistic many-particle situations, the BH forms much later (because usually, a huge number of particles is necessary for the actual BH creation) and decays earlier (it seems reasonable to assume that a too-low number of particles is unable to support the existence of the BH). Anyway, when a state (for some  $k$  close to  $n$ , i.e., for the final stages of BH evolution) quitting the upper box  $U_{k-1}^{(1)}$  (potentially belonging to a BH) is the vacuum state  $(|\psi_k\rangle^{(1)} = |0\rangle^{(1)})$ , i.e., the total state  $|\psi_k\rangle$  assumes the particular (product) form  $|\psi_k\rangle = |0\rangle^{(1)} \otimes |\psi_k\rangle^{(2)}$ , certainly, the BH already (at this stage  $k$ ) does not exist (has evaporated)—the vacuum state  $|0\rangle^{(1)}$  cannot support the existence of the BH. Consequently, the rest of the unitary operators (corresponding to  $i = k, k+1, \dots, n-1$ ) ceases to be essential from the point of view of the BH evolution (evaporation) and thus can be put in the trivial form  $U_i = \mathbb{I}$  or (equivalently) can be simply skipped.

### 3.1 Product models

The product models discussed in this subsection are tensor products ( $m$ -th tensor powers) of the 3Q model defined in Subsubsection 3.1.1. Obviously,  $m$ -th tensor powers are algebraically unique for a given  $m$ , but as will be observed in Subsubsection 3.1.2, as far as the (semi)causal structure is concerned, there is a multitude of different product models for each  $m$ . From combinatorics, it follows that there are precisely  $2^{-m}$  ( $2m$ )! models for a given  $m$ , which in general can yield different entropy curves.

#### 3.1.1 Three-qubit model

The three-qubit (3Q) model first appeared (rather sketchy and in “a four-qubit incarnation”) in the context of firewalls in [17] and then directly and explicitly in [6]. Another but akin version of the 3Q model was proposed and discussed in [7] (see also [8]), whereas its some four-qubit extension in [9]. In this Subsubsection, the 3Q model appears for pedagogical reasons as well as an elementary building block for our further constructions. Our present approach closely follows [7].

The 3Q model can be concisely described in terms of a quantum circuit, as presented in Figure 6. In the notation of (6) (see Figure 3), the unitary evolution  $U$  of the 3Q model assumes the following block structure

$$U = U_3 U_2 U_1 U_0 \equiv U_3 \left( U_2^{(1)} \otimes U_2^{(2)} \right) \left( U_1^{(1)} \otimes U_1^{(2)} \right) U_0. \quad (23)$$

Here the first unitary block  $U_0$  implements the Hawking process on the second and third qubit, followed by a swap operation on the first and third one,  $U_1 = U_3 = \mathbb{I}$  (identity), and  $U_2 = U_2^{(1)} \otimes U_2^{(2)}$ , where  $U_2^{(1)}$  can be interpreted as an inverse of the Hawking process and  $U_2^{(2)} = \mathbb{I}$ .

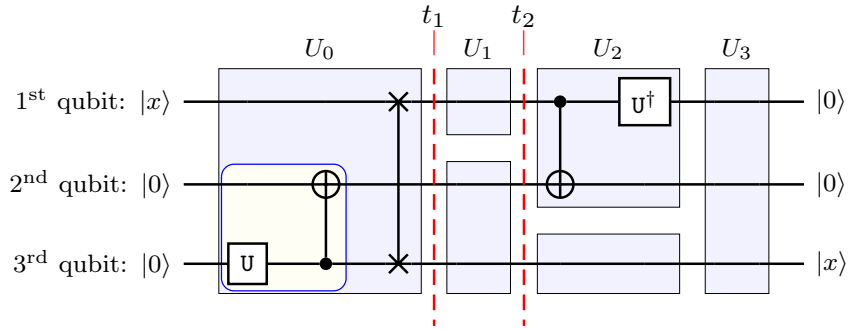


Fig. 6: (Color online) Quantum circuit defining the three-qubit (3Q) model. The first qubit, in the state  $|x\rangle$ , is interpreted as a ‘‘matter’’ qubit entering the BH, whereas the other two (vacuum) qubits are utilized for Hawking particle production. The Hawking effect parametrized by  $U$  takes place in the rounded box (see (25)) in the left lower corner of the circuit.

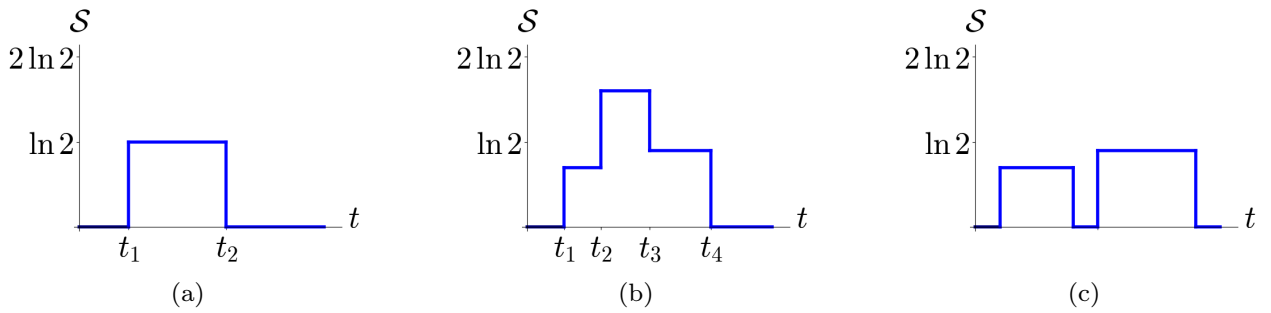


Fig. 7: (Color online) Example entropy curves for the simplest few-qubit product models. (a) Possible evolution of entanglement entropy for the three-qubit (3Q) model. In this particular example, in the time interval between  $t_1$  and  $t_2$ , the entropy attains its (maximum) value  $S = \ln 2$  ( $t_1$  and  $t_2$  are defined in Figure 6). In general, i.e., for arbitrary  $U$ ,  $0 \leq S \leq \ln 2$ . (b) Possible evolution of entanglement entropy for the tensor square of the three-qubit ( $3Q^2$ ) model. The entropy curve belongs to ‘‘the Page type’’ (the cases (1)–(4) on the list (29)). In particular, for  $S_1 = S_2 = \ln 2$  (the extremal case), we would exactly obtain ‘‘the two-qubit Page curve’’.  $t_1, t_2, t_3$ , and  $t_4$  are defined in Figure 8. (c) Another type of possible evolution of entanglement entropy for the  $3Q^2$  model. This time the curve is ‘‘minimal’’ rather than of ‘‘the Page type’’—the cases (5)–(6) on the list (29).

In principle, the one-qubit operator  $U$  in Figure 6 could be an arbitrary unitary operator, but we can as well assume that it is orthogonal, given in the form

$$U = U_{r_p} = \begin{pmatrix} \cos r_p & -\sin r_p \\ \sin r_p & \cos r_p \end{pmatrix}, \quad (24)$$

because of the correspondence to the Hawking process for fermions, described by orthogonal (Bogolyubov) transformations. More precisely, the gate

implements the (one-mode  $p$ ) Hawking process for fermions with mass  $m$  and momentum  $p$ , where

$$\cos r_p = [2 \cosh(\pi \omega_p / \kappa)]^{-1/2} \exp(\pi \omega_p / 2\kappa), \quad \omega_p = \sqrt{p^2 + m^2}, \quad (26)$$

with  $\kappa$  denoting the surface gravity [18].

In the 3Q model, the entanglement entropy  $S$  only changes at the instants  $t_1$  (there is a jump of the numeric value of  $S$  from 0 to some non-negative value  $S \leq \ln 2$ ) and  $t_2$  (a jump from the value  $S$  to 0 back), as depicted in Figure 7a ( $t_1$  and  $t_2$  are defined in Figure 6). In terms of the four blocks  $U_0, \dots, U_3$  of Figure 6, the evolution of entanglement entropy proceeds according to the pattern

$$0 \xrightarrow{0} S \xrightarrow{1} 0 \xrightarrow{2} 0 \xrightarrow{3}, \quad (27)$$

where the underscripts number the unitary blocks. The evolution of entropy can be called extremal, if the entropy attains its maximal allowed value, i.e., for this model  $S = \ln 2$ . According to (26) this happens in the limit of  $\kappa \rightarrow \infty$  or  $\omega_p (= \sqrt{p^2 + m^2}) \rightarrow 0$  (maximal entanglement, see (25)).

### 3.1.2 Tensor square of the three-qubit model

As an intermediate stage between the 3Q model and its arbitrary  $m$ -th tensor power ( $3Q^m$ ), we will consider the  $3Q^2$  model, which is a tensor square of the 3Q model. The  $3Q^2$  model operates on six qubits, and its unitary evolution  $U$  can be semicausally decomposed into  $1 + 6$  (number of qubits) = 7 blocks

$$\begin{aligned} U = & U_6 U_5 U_4 U_3 U_2 U_1 U_0 \\ \equiv & U_6 \left( U_5^{(1)} \otimes U_{n-1}^{(2)} \right) \dots \left( U_2^{(1)} \otimes U_2^{(2)} \right) \left( U_1^{(1)} \otimes U_1^{(2)} \right) U_0. \end{aligned} \quad (28)$$

One of the versions of the model (a preferred one from our perspective) is explicitly presented in Figure 8. As already mentioned at the beginning of Subsection 3.1, even though from a purely algebraic

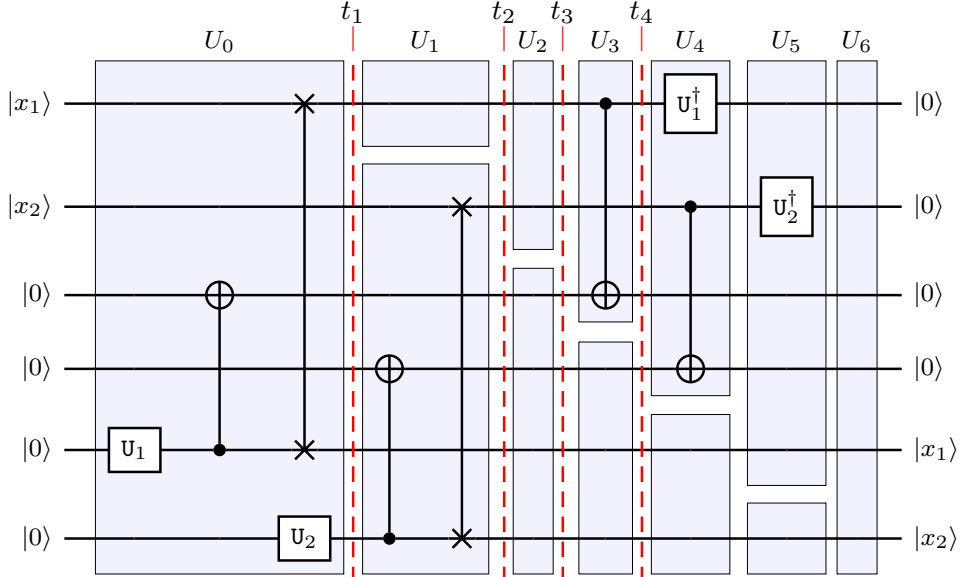


Fig. 8: (Color online) Quantum circuit defining one of the 6 variants of the  $3Q^2$  model (the first case on the list of possible semicausal embeddings (29)). The first two qubits, in the states  $|x_1\rangle$  and  $|x_2\rangle$ , are interpreted as “matter” qubits entering the BH, whereas the other four (vacuum) qubits are utilized for Hawking particle production.

point of view the tensor square (and more generally, the tensor power) is unique, the corresponding models are not, because of various possibilities of embeddings in the surrounding semicausal frame (Figure 3). That follows from the fact that particular qubits can enter successive upper subboxes  $(U_1^{(1)}, U_2^{(1)}, \dots, U_{n-1}^{(1)}, U_n)$  in various orders, giving rise to (in principle) different entropy curves. For the  $3Q^2$  model, we have six possibilities, which can be identified by the following entropy jumps:

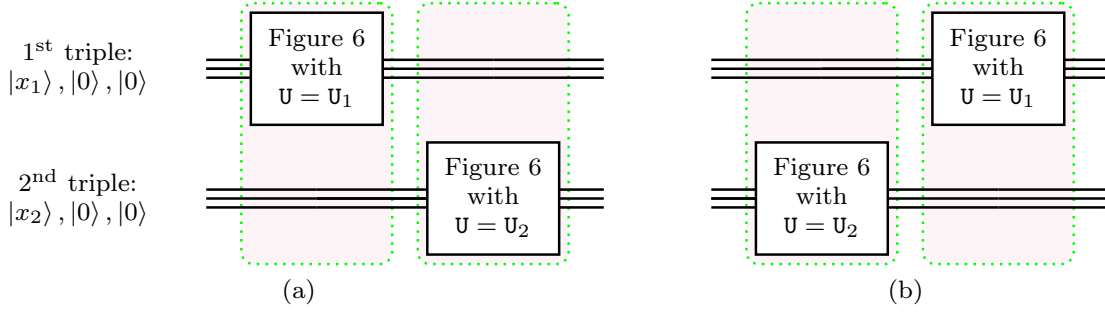


Fig. 9: (Color online) Schematic presentation of quantum circuits defining the last two cases on the list (29) of all possible semicausal embeddings of the  $3Q^2$  model. The cases (5) and (6), depicted in (a) and (b), respectively, belong to the “minimal” (or “decoupled”) type, i.e., the shape of their entropy curves is similar to the shape of the curve depicted in Figure 7c.

- (1)  $0 \xrightarrow{1} S_1 \xrightarrow{2} S_1 + S_2 \xrightarrow{3} S_2 \xrightarrow{4} 0 \xrightarrow{5} 0 \xrightarrow{6} 0;$
- (2)  $0 \rightarrow S_1 \rightarrow S_1 + S_2 \rightarrow S_1 \rightarrow 0;$
- (3)  $0 \rightarrow S_2 \rightarrow S_1 + S_2 \rightarrow S_1 \rightarrow 0;$
- (4)  $0 \rightarrow S_2 \rightarrow S_1 + S_2 \rightarrow S_2 \rightarrow 0;$
- (5)  $0 \rightarrow S_1 \rightarrow 0 \rightarrow S_2 \rightarrow 0;$
- (6)  $0 \rightarrow S_2 \rightarrow 0 \rightarrow S_1 \rightarrow 0.$

(29)

The first case (1) on the list (29) (with explicitly numbered blocks  $U_0, \dots, U_6$  by the underscripts 0, 1, ..., 6) corresponds to the model presented in Figure 8, and its entropy jumps are qualitatively illustrated in Figure 7b; the second case (2) is some variation of (1); the cases (3) and (4) are “qubit transpositions” of (1) and (2), respectively; whereas the cases (5) and (6) are “causally decoupled” models. The cases (1)–(4) belong to “the Page type”, i.e., the shape of their entropy curves resembles the shape of the curve depicted in Figure 7b; in particular, for  $S_{1,2} = \ln 2$  (the extremal case), we exactly obtain “the two-qubit Page curve”. The cases (5) and (6) schematically presented in Figure 9a and Figure 9b, respectively, belong to the “minimal” type, i.e., the shape of their entropy curves resembles the shape of the curve depicted in Figure 7c.

One should also note that  $S_1$  and  $S_2$  ( $0 \leq S_{1,2} \leq \ln 2$ ) are contributions to the entanglement entropy  $\mathcal{S}$  coming from the Hawking effect rather than from the “matter” qubits  $|x_1\rangle$  and  $|x_2\rangle$ .

### 3.1.3 Arbitrary tensor power of the three-qubit model

From the point of view of entropy curves (or entropy evolution), various  $3Q^m$  models with the fixed tensor power  $m$  can be characterized by various series of entropy contributions  $\pm S_1, \pm S_2, \dots, \pm S_m$ , where the numeric values  $S_i$  ( $0 \leq S_i \leq \ln 2$ ,  $i = 1, 2, \dots, m$ ) of the entanglement entropy  $\mathcal{S}$  depend on the explicit form of the corresponding  $U(2)$  matrices  $U_i$ . For example, the subset of all  $3Q^m$  models corresponding to entropy jumps (analogous to the cases (1)–(4) on the list (29))

$$\begin{aligned}
 0 &\rightarrow S_{\sigma_+(1)} \rightarrow S_{\sigma_+(1)} + S_{\sigma_+(2)} \rightarrow \dots \rightarrow S_{\sigma_+(1)} + S_{\sigma_+(2)} + \dots + S_{\sigma_+(m)} \\
 &\rightarrow S_{\sigma_+(1)} + S_{\sigma_+(2)} + \dots + S_{\sigma_+(m)} - S_{\sigma_-(1)} \\
 &\rightarrow S_{\sigma_+(1)} + S_{\sigma_+(2)} + \dots + S_{\sigma_+(m)} - S_{\sigma_-(1)} - S_{\sigma_-(2)} \rightarrow \dots \rightarrow 0,
 \end{aligned}
 \tag{30}$$

where  $\sigma_+$  and  $\sigma_-$  are two independent permutations of  $m$  elements, is of “the Page type”, i.e., for  $S_i \approx \ln 2$  the shape of the entropy curves for these models is similar to the shape of the curve depicted

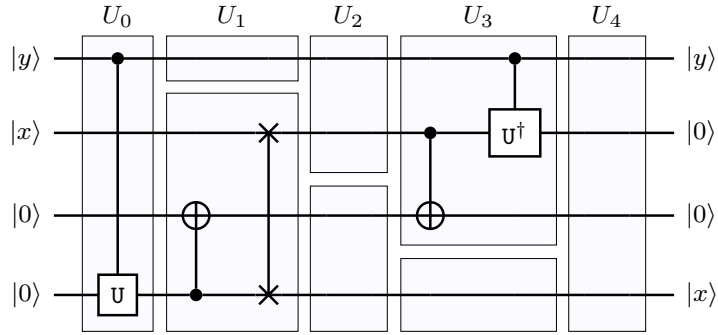


Fig. 10: Quantum circuit defining the controlled three-qubit (C3Q) model. The first two qubits, in the states  $|y\rangle$  (a control qubit) and  $|x\rangle$ , are “matter” qubits, whereas the other two vacuum states are utilized for Hawking particle production. In the first unitary block ( $U_0$ ) the qubit  $|y\rangle$  controls the Hawking effect by the CNOT-U gate determined by the  $U(2)$  matrix  $U$ .

in Figure 5b or Figure 5c for  $m \gg 1$  (two upper edges of the triangle). Instead, the subset of  $3Q^m$  models corresponding to entropy jumps (analogous to the cases (5)–(6) in (29))

$$0 \rightarrow S_{\sigma(1)} \rightarrow 0 \rightarrow S_{\sigma(2)} \rightarrow 0 \rightarrow \cdots \rightarrow 0 \rightarrow S_{\sigma(m)} \rightarrow 0, \quad (31)$$

where  $\sigma$  is a (single) permutation of  $m$  elements, belongs to the “minimal” type, i.e., for  $m \gg 1$  their entropy curves are very close to the lower (dashed) edge of the (shaded) triangle in Figure 5c. Let us also note that the number of models belonging to the Page type (30) is equal to  $(m!)^2$ , and for  $m \gg 1$  this number is much larger than the number of “minimal” models (31), which is equal to  $m!$ .

### 3.2 Non-product models

A lot of (product) models introduced in the previous Subsection 3.1 can yield entropy curves arbitrarily close to the Page curve, but from the point of view of physics, the models can seem to be almost trivial—interactions are bounded to mutually isolated and almost identical (i.e., possibly differing only by one-qubit operators  $U_i$  or equivalently by the parameters  $r_{p_i}$  in (24)) three-qubit sectors. The Hawking process in these models is determined by the fixed family of matrices  $\{U_i\}_{i=1}^m$ . Therefore, the whole system looks like an *open* one defined by externally prescribed  $r_{p_i}$ ,  $i = 1, 2, \dots, m$ . To remove these limitations, in this subsection we introduce a family of controlled non-product models, which are controlled with a relatively small set of  $l$  control qubits  $\{|y_i\rangle\}_{i=1}^l$ . The control qubits should be interpreted as the part of all “matter” qubits that gradually enter the BH, but their modest number is unable to support the existence of the BH in the final stages of its evolution. Thus, the total number of qubits in these models amounts to  $n = l + 3m$  ( $l$  control qubits and  $3m$  “controlled” qubits, including  $m$  “matter” qubits as well as  $2m$  Hawking ones), where for large  $m$  (the case of BHs), we should assume that  $l \ll m$ . The simplest case,  $l = 1$  and  $m = 1$ , i.e., the controlled three-qubit (C3Q) model, is discussed in the following Subsubsection 3.2.1, whereas the case of arbitrary  $l$  and  $m$ , i.e., the  $l$ -controlled  $3m$ -qubit ( $lC3mQ$ ) model, is introduced in Subsubsection 3.2.2.

#### 3.2.1 The controlled three-qubit model

The controlled three-qubit (C3Q) model operates on four qubits (see Figure 10): two “matter” qubits in arbitrary states  $|y\rangle$  (a control qubit) and  $|x\rangle$  as well as two “Hawking qubits”, initially both in the vacuum state  $|0\rangle$ . The model is parameterized by a single one-qubit  $U(2)$  matrix  $U$ , possibly limited to the orthogonal (Bogolyubov–Hawking) form (24). The qubit  $|y\rangle$  controls (according to the NOT-rule) the Hawking effect by the CNOT-U gate in the block  $U_0$  of Figure 10.

The evolution of the entanglement entropy  $\mathcal{S}$  proceeds in consecutive blocks  $U_0, \dots, U_4$ , according to the pattern (compare to (27))

$$0 \rightarrow \begin{smallmatrix} S' \\ 1 \end{smallmatrix} \rightarrow \begin{smallmatrix} S'' \\ 2 \end{smallmatrix} \rightarrow \begin{smallmatrix} 0 \\ 3 \end{smallmatrix} \rightarrow \begin{smallmatrix} 0 \\ 4 \end{smallmatrix}, \quad (32)$$

where the numeric values of  $S$ , i.e.,  $S'$  and  $S''$ , with  $0 \leq S', S'' \leq \ln 2$ , are determined by the qubit  $|y\rangle$  and the explicit form of the matrix  $U$ . One should remark that the contributions  $S'$  and  $S''$  are coming from the Hawking particles as well as from the control “matter” qubit  $|y\rangle$ .

Let us note that some immediate and natural generalization of the C3Q model is possible by the replacement of the CNOT- $U$  gate (defined with a single  $U(2)$  matrix  $U$ ) in the block  $U_0$  of Figure 10 by a gate determined with a pair of  $U(2)$  matrices  $U_1$  and  $U_2$ , i.e., for the whole two-qubit unitary operator, we have the generalization

$$\begin{pmatrix} \mathbb{I} & 0 \\ 0 & U \end{pmatrix} \rightarrow U \equiv \begin{pmatrix} U_1 & 0 \\ 0 & U_2 \end{pmatrix}, \quad (33)$$

where the matrices  $U_1$  and  $U_2$  correspond to the control qubits  $|0\rangle$  and  $|1\rangle$ , respectively.

### 3.2.2 Controlled multiqubit models

The  $l$ -controlled  $3m$ -qubit ( $lC3mQ$ ) model is a direct generalization of the C3Q model of the previous subsubsection, where instead of a single control qubit  $|y\rangle$  we have a (small) set of  $l$  control qubits  $|y_1\rangle, |y_2\rangle, \dots, |y_l\rangle$ , and instead of a single triple of the controlled qubits (initially in the states  $|x\rangle, |0\rangle, |0\rangle$ ) we have a set of  $m$  triples (initially in the states  $|x_1\rangle, |0\rangle, |0\rangle, \dots, |x_m\rangle, |0\rangle, |0\rangle$ ). Then, the total number of qubits amounts to  $n = l + 3m$ . Moreover, for each triple  $i$  ( $i = 1, 2, \dots, m$ ) there is defined a collection of the  $2^l$   $U(2)$  matrices  $\{U_j(i)\}_{j=1}^{2^l}$  that determine an  $l + 1$ -qubit unitary matrix  $U_i$  of dimension  $2^{l+1} \times 2^{l+1}$ —a generalization of (33) to  $l$  control qubits. Explicitly,

$$U_i = \begin{pmatrix} U_1(i) & & & 0 & & \\ & U_2(i) & & & & \\ & & \ddots & & & \\ 0 & & & & & U_{2^l}(i) \end{pmatrix}, \quad (34)$$

where the  $U(2)$  matrices  $U_j(i)$  operate in the  $i$ -th qubit triple and binary presentation of the number  $j$  corresponds to the series of “control” digits given by  $y_1 \dots y_l$ .

The general structure of the  $lC3mQ$  model is schematically depicted in block form in Figure 11. The whole family of the models is parametrized by  $m$   $2^l$ -element collections of  $U(2)$  matrices  $\{U_j(i)\}_{j=1}^{2^l}$ ,  $i = 1, \dots, m$ , and by a multitude of various semicausal structures. By virtue of the construction, entropy curves are still within the semicausal entropy bound given in (21) and described in Subsubsection (2.2.1), but they in a more complicated way depend on the matrices  $U_j(i)$  as well as on the initial values of the control “matter” qubits  $|y_1\rangle, \dots, |y_l\rangle$ .

### 3.3 Black hole physics in qubit models

Our models incorporate all principal stages of standard classical and quantum evolution from the point of view of BH physics. The first era, BH formation, is based on “matter” qubits represented by  $|x\rangle, |y\rangle, |x_i\rangle$  ( $i = 1, 2, \dots, m$ ), and  $|y_k\rangle$  ( $k = 1, 2, \dots, l$ ) in the models of Subsubsection 3.1.1, 3.2.1, 3.1.3, and 3.2.2, respectively. These qubits represent all incoming particles that create the BH through standard classical gravitational collapse. The second era, BH (quantum) evaporation and disappearance, involves the Hawking process of particle pair-production. All models include the Hawking mechanism through gate (25), which yields the entangled state  $\cos r_p |00\rangle + \sin r_p |11\rangle$  and formally implements Hawking pair creation for a fermion mode with mass  $m$  and momentum  $p$ . The parameters  $m$  and  $p$  defining gate (25) are determined by (26) and (24). We associate qubit  $|0\rangle$  with the vacuum state and qubit  $|1\rangle$  with a one-particle state, as explained in the second-to-last paragraph of Section 3’s beginning part.

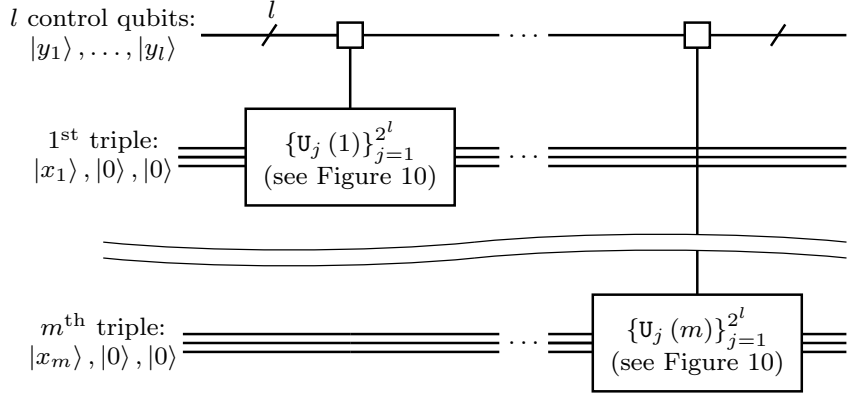


Fig. 11: Schematic presentation (in block form) of the quantum circuit for the  $l$ -controlled  $3m$ -qubit ( $lC3mQ$ ) model without explicitly imposed semicausal structure. The model operates on  $n$  ( $= l + 3m$ ) qubits, where for each qubit triple  $\{|x_i\rangle, |0\rangle, |0\rangle\}$  ( $i = 1, 2, \dots, m$ ), there is an associated collection of the  $2^l$   $U(2)$  matrices  $\{U_j(i)\}_{j=1}^{2^l}$  that define an  $l + 1$ -qubit unitary operator  $U_i$  of the form (34). The matrices  $U_1(i), U_2(i), \dots, U_{2^l}(i)$  act on a single qubit in the box corresponding to the given  $i$ -th triple.

Our models function as toy models, without a specific Hamiltonian or action. Loosely speaking, the systems represented by our product models (Subsection 3.1) can be viewed as qubit analogs of uncoupled oscillators. Non-product models (Subsection 3.2), on the other hand, can be seen as analogous to specifically coupled oscillators. It is important to note that there is no widely agreed upon detailed scenario for the final moments of BH evolution (evaporation), and therefore various possibilities could be considered. In our product models, the transition of the state inside either box  $U^{(X_1 X_2 \dots X_{N-1})}$  in Figure 2 or box  $U_{n-1}^{(1)}$  in Figure 3 to the "vacuum" state indicates a peaceful disappearance of the BH. As discussed in the final paragraph of the paper, in non-product models, we assume that a small number of control qubits are released only after the BH has completely ceased to exist, as too few particles are unable to sustain the BH's existence.

#### 4 Summary and final remarks

Utilizing the universal form of semicausal evolution (1) (see Figure 1a), we have established a general structure of the quantum circuit presenting unitary evolution and respecting causality imposed by the BH event horizon (see Figures 3 and 4). Moreover, making use of several standard properties of the von Neumann entropy (the triangle inequality, isometric invariance, and others), we have determined principles governing the evolution of the corresponding BH entanglement entropy (see (15) and (21)), and next visualized them in Figure 5 as well as additionally summarized in Subsubsection 2.2.1.

In the second part of the work (Section 3), for illustration purposes, two multiparametric families of unitary semicausal qubit toy models have been considered: tensor product models ( $3Q^m$  models) and controlled non-product models ( $lC3mQ$  models). By virtue of the construction of the  $3Q$  model (Figure 6), the role played by individual qubits and consequently the direction of the flow of information are rather clear. In particular, we can state that "external information" carried by the  $1^{\text{st}}$  qubit (a "matter" qubit in the state  $|x\rangle$ ) is exchanged by the swap gate with that in the outgoing Hawking qubit (the  $3^{\text{rd}}$  qubit in the box  $U_0$ ). Therefore, evidently, in the  $3Q^m$  models, Hawking radiation produces BH entropy. In turn, at the latter stages of BH evolution, the accumulated BH entropy is gradually being cancelled by the partner qubits of the Hawking pairs (see the  $2^{\text{nd}}$  qubit in box  $U_2$ ). In other words, "truly external" (carried by the  $1^{\text{st}}$  qubit) information does not cross the BH horizon and is (therefore) not lost. In Subsection 3.2, to "dynamically close" the system, we have introduced the controlled non-product models with a limited number of  $l$  (external) control qubits, which serve to parameterize the Hawking effect. Since the control qubits are supposed to enter the BH as well as to be later finally released, in these models, we are forced to (additionally, but hopefully reasonably) assume that a very

small number of particles is unable to support the existence of the BH, and therefore the BH has to decay and free the rest of particles (exactly, the control matter particles). Presumably, such a physics scenario could be conceivable for the total mass of all  $l$  control particles less than the Planck mass, i.e.,  $M_{l\text{ control}} < M_{\text{Planck}}$ . Consequently, in the controlled non-product models, a small contribution to the BH entropy also comes from the control matter particles.

## References

1. S. W. Hawking. Breakdown of predictability in gravitational collapse. *Physical Review D*, 14: 2460–2473, November 1976. doi: 10.1103/PhysRevD.14.2460. URL <https://link.aps.org/doi/10.1103/PhysRevD.14.2460>.
2. Ahmed Almheiri, Netta Engelhardt, Donald Marolf, and Henry Maxfield. The entropy of bulk quantum fields and the entanglement wedge of an evaporating black hole. *Journal of High Energy Physics*, 2019(12):63, December 2019. doi: 10.1007/JHEP12(2019)063.
3. Geoffrey Penington. Entanglement wedge reconstruction and the information paradox. *Journal of High Energy Physics*, 2020(9):2, September 2020. doi: 10.1007/JHEP09(2020)002.
4. Don N. Page. Information in black hole radiation. *Physical Review Letters*, 71:3743–3746, December 1993. doi: 10.1103/PhysRevLett.71.3743. URL <https://link.aps.org/doi/10.1103/PhysRevLett.71.3743>.
5. Steven G. Avery. Qubit Models of Black Hole Evaporation. *Journal of High Energy Physics*, 01: 176, 2013. doi: 10.1007/JHEP01(2013)176.
6. Kento Osuga and Don N. Page. Qubit transport model for unitary black hole evaporation without firewalls. *Physical Review D*, 97:066023, March 2018. doi: 10.1103/PhysRevD.97.066023. URL <https://link.aps.org/doi/10.1103/PhysRevD.97.066023>.
7. Bogusław Broda. Unitary toy qubit transport model for black hole evaporation. *The European Physical Journal C*, 80(5):418, May 2020. doi: 10.1140/epjc/s10052-020-7947-1.
8. Bogusław Broda. Fermionic model of unitary transport of qubits from a black hole. *Physical Review D*, 103:025022, January 2021. doi: 10.1103/PhysRevD.103.025022. URL <https://link.aps.org/doi/10.1103/PhysRevD.103.025022>.
9. Bogusław Broda. Causal unitary qubit model of black hole evaporation. *Physics Letters B*, 820: 136564, September 2021. doi: 10.1016/j.physletb.2021.136564.
10. David Beckman, Daniel Gottesman, M. A. Nielsen, and John Preskill. Causal and localizable quantum operations. *Physical Review A - Atomic, Molecular, and Optical Physics*, 64, 2001. ISSN 10941622. doi: 10.1103/PhysRevA.64.052309.
11. T. Eggeling, D. Schlingemann, and R. F. Werner. Semicausal operations are semilocalizable. *Europhysics Letters*, 57, 2002. ISSN 02955075. doi: 10.1209/epl/i2002-00579-4.
12. M. Piani, M. Horodecki, P. Horodecki, and R. Horodecki. Properties of quantum nonsignaling boxes. *Physical Review A - Atomic, Molecular, and Optical Physics*, 74, 2006. ISSN 10502947. doi: 10.1103/PhysRevA.74.012305.
13. Benjamin Schumacher and Michael D. Westmoreland. Isolation and Information Flow in Quantum Dynamics. *Foundations of Physics*, 42, 2012. ISSN 00159018. doi: 10.1007/s10701-012-9651-y.
14. Benjamin Schumacher and Michael D. Westmoreland. Locality and information transfer in quantum operations. *Quantum Information Processing*, 4, 2005. ISSN 15700755. doi: 10.1007/s11128-004-3193-y.
15. Samuel L. Braunstein and Stefano Pirandola. Quantum information versus black hole physics: Deep firewalls from narrow assumptions. *Philosophical Transactions of the Royal Society A: Mathematical, Physical and Engineering Sciences*, 376, 2018. ISSN 1364503X. doi: 10.1098/rsta.2017.0324.
16. Huzihiro Araki and Elliott H Lieb. Entropy inequalities. *Communications in Mathematical Physics*, 18(2):160–170, 1970.
17. Ahmed Almheiri, Donald Marolf, Joseph Polchinski, Douglas Stanford, and James Sully. An Apologia for Firewalls. *Journal of High Energy Physics*, 09:018, 2013. doi: 10.1007/JHEP09(2013)018.

18. Robert B. Mann. *Black Holes: Thermodynamics, Information, and Firewalls*. Springer-Briefs in Physics. Springer, 2015. ISBN 978-3-319-14495-5, 978-3-319-14496-2. doi: 10.1007/978-3-319-14496-2.

**Acknowledgements** This work was supported by the University of Łódź.